Colloid Polym Sci (2017) 295:2423–2431
https://doi.org/10.1007/s00396-017-4218-2

ORIGINAL CONTRIBUTION

Effects of hydrophilic groups of curing agents on the properties of flame-retardant two-component waterborne coatings

Xuan Yin[1] · **Chenghao Dong**[1] · **Yunjun Luo**[1]

Received: 28 August 2017 / Revised: 9 October 2017 / Accepted: 16 October 2017 / Published online: 31 October 2017

Abstract A novel hydrophilic curing agent was prepared through hexamethylene diisocyanate trimer, polyethylene glycol monomethyl ether, and 2-((2-aminoethyl)amino)-ethanesulfonic acid monosodium salt. Then, flame-retardant two-component waterborne polyurethanes and their coatings were synthesized through adding the novel hydrophilic curing agent. Their properties and analysis were characterized through fourier-transformed infrared spectroscopy, differential scanning calorimeter, thermogravimetric, thermogravimetric infrared, limiting oxygen index, and UL-94. As a result, the −NCO content of novel hydrophilic curing agent was 16.4% and above 10.0% about 4 months. Besides, the novel hydrophilic curing agent dispersed well in two-component emulsions and improved themostability and compatibility of two-component flame-retardant waterborne polyurethanes. Meanwhile, the tensile strength of the novel film was 1.5 times than the previous one through adding novel hydrophilic curing agent at the same stoichiometric ratio of −NCO to −OH. What's more, the best LOI and UL-94 of modified flame-retardant two-component waterborne polyurethane were 29.2% and V-0, respectively.

Keywords Cross-linking · Polyurethanes · Flame retardancy · Degradation · Properties, thermal · Coatings

✉ Yunjun Luo
yjluo@bit.edu.cn

[1] School of Materials Science and Engineering, Beijing Institute of Technology, Beijing 100081, People's Republic of China

Introduction

Two-component waterborne polyurethane (2K-WPU) consists of hydroxyl component and isocyanate component. For the hydroxyl component, the structure is easily controlled [1]; but for the isocyanate component, it reacts with hydrophilic molecules to create cross-linking to cure film. 2K-WPU is a combustible material and bound to pose a potential fire hazard if it is not modified with flame retardants. For this reason, the modification of 2K-WPU could effectively reduce the occurrence of fire during manufacturing. It is worth noting that 2K-WPU has non-toxic and weather resistant through chemical synthesis [2–4]. Therefore, researching 2K-WPU has important implication and practical application values in terms of modification via flame retardant and hydrophilic curing agent.

Organic phosphorus flame retardants and phosphorus-nitrogen flame retardants have attracted great deal of research attentions [5]. Halogen-free poly-phosphate (OP550) is a phosphorus-nitrogen flame retardant, which acts through forming non-volatile protective film composed of phosphoric or polyphosphoric acid to isolate combustible gases. Meanwhile, phosphorus-oxygen-free groups react with reactive hydrogen and hydroxide groups and further inhibit combustibility during heating. Polyurethane polyols react with curing agent to synthesize cross-linked polyurethane which shows good weather resistance and photostability. These technologies of preparing hydrophilic curing agent have been crucial for developing direction in Bayer, BASF, and other key enterprises, especially Jacobs, who first broke the unhydrophilic barriers of isocyanate [6]. Bayer initially modified hydrophilic curing agent to obtain more −NCO groups. Compared with the hexamethylene diisocyanate (HDI) curing agent modified through polyether, the one modified through sulphonate could provide enduring water resistance and low viscosity for films after alkaline neutralization [7]. Therefore,

the main method of propagating hydrophilic curing agent is to import hydrophilic groups into macromolecule structure such as polyethylene glycol monomethyl ether or aminosulphonate. We used these two modifications to prepare a hydrophilic curing agent to obtain better film property.

This paper reported a hydrophilic curing agent (we took out a patent [8]), and then prepared a hydroxyl component (according to previous research [9]). Hereafter, we prepared four flame-retardant two-component waterborne polyurethanes and their films. The novel hydrophilic curing agent had good stability and high −NCO content. And the thermostability and flame retardancy of flame-retardant two-components were improved by novel hydrophilic curing agent.

Experimental

Materials

Hexamethylene diisocyanate tripolymer (HDI trimer, industrial grade, storage without using water, Bayer Co.); polyethylene glycol monomethyl ether (PGME, $\overline{M_n} = 500$, chemically pure, Shanghai Yiji Chemical Engineering Co., Ltd.) was dried under vacuum at 80 °C for 12 h; 2-((2-aminoethyl)amino)-ethanesulfonic acid monosodium salt (AAS salt, 99%,Bayer Co.) was dried under vacuum at 85 °C for 6 h; PPG1000 ($\overline{M_n} = 1000$, industrial grade, Dawson International Inc.) was dried under vacuum at 90 °C for 6 h; isophorone diisocyanate (IPDI, analytical grade, Aladdin); dimethylol propionic acid (DMPA, chemically pure, Aladdin) was dried under vacuum at 90 °C for 6 h; halogen-free poly-phosphate (OP550, $\overline{M_n} = 831$, industrial grade, Clariant AG) was dried under vacuum at 90 °C for 4 h; acetone (chemically pure, Beijing Chemical Reagents Company) was dried over a 4Å molecular sieve (Beijing Pengcai Chemical Reagent Co., Ltd.) for 72 h; triethylamine (TEA, chemically pure, Beijing Yili Fine Chemicals Co., Ltd.) was soaked by 4Å molecular sieve for 72 h; hydrophilic curing agent (Lab homemade [8]); antifoaming agent (BYK 001, chemically pure, BYK Additives & Instruments) was dried under vacuum at 80 °C for 4 h; wetting agent (BYK348, chemically pure, BYK Additives & Instruments) was dried under vacuum at 80 °C for 4 h; flow control agent (BYK333, chemically pure, BYK Additives & Instruments) was dried under vacuum at 80 °C for 4 h.

Methods

Synthesis of hydrophilic curing agent

HDI trimer and PGMG (weight ratio 20:3) were dropped into 100-mL four-neck flask with condenser pipe, and stirred at 75 °C for 4 h. Subsequently, the temperature was cooled to 25 °C. AAS salt (weight ratio of HDI trimer and AAS salt was between 50:1 and 50:4) was dropwise added into the reaction through constant pressure funnel. Besides, the whole reaction was under nitrogen atmosphere. The synthesis of the hydrophilic curing agent (named M12A4) is displayed in Scheme 1 [10].

Preparation of two-component waterborne polyurethane coatings

100.0 g PPG1000, 27.0 g OP550, and 41.8 g IPDI were added into 250-mL four-neck flask with condenser pipe, and stirred at 80 °C for 2 to 3 h. Then 9.9 g DMPA and some acetone were added, and the mixture was stirred for another 1 to 2 h. Subsequently, the temperature was cooled to 40 °C. Next, 9.9 g TEA was added into the reaction vessel for 30 min to obtain prepolymer which was mixed with 376.0 g deionized water at high-speed shear mixing for 30 min. A hydroxyl-terminated polyurethane emulsion was obtained after removal of acetone from the emulsion at 40 °C for 2 h by rotary vacuum evaporation under reduced pressure. The hydrophilic curing agent (MHP15 or M12A4 hydrophilic curing agent) was added (the stoichiometric ratio of −NCO to −OH was 1.4 and 1.6, respectively) into the emulsion with 0.3 g antifoaming agent, 0.45 g wetting agent, and 0.75 g flow control agent, which was under ultrasonic vibration for 30 min to wait for complete reaction. Finally, the resultant emulsion was two-component flame-retardant waterborne polyurethane. The two-component waterborne polyurethanes with 1.4 and 1.6 for stoichiometric ratio of −NCO to −OH and MHP15 were named MWPU-1 and MWPU-2, respectively, and the two-component waterborne polyurethanes with 1.4 and 1.6 for stoichiometric ratio of −NCO to −OH and M12A4 were named MAWPU-1 and MAWPU-2, respectively. The synthesis is similar with previous research [7]. The MWPU and MAWPU were dropped into a Teflon plate at 60 °C for 48 h to obtain films on vacuum drying oven.

Characterization

Hydrophilic curing agent and its emulsion

The Nicolet 8700 Fourier transformed infrared spectroscopy (FTIR, Thermo Nicolet Corporation, Waltham, USA) was used to test the final resultants.

−NCO content. −NCO values were tested according to standard HG-T2409-1992. The −NCO value was calculated on the basis of the formula (1).

$$-\mathrm{NCO}\% = \frac{(V_1 - V_2) \times c \times 0.0420}{m} \times 100\% = \frac{(V_1 - V_2) \times c}{m} \times 4.2\% \quad (1)$$

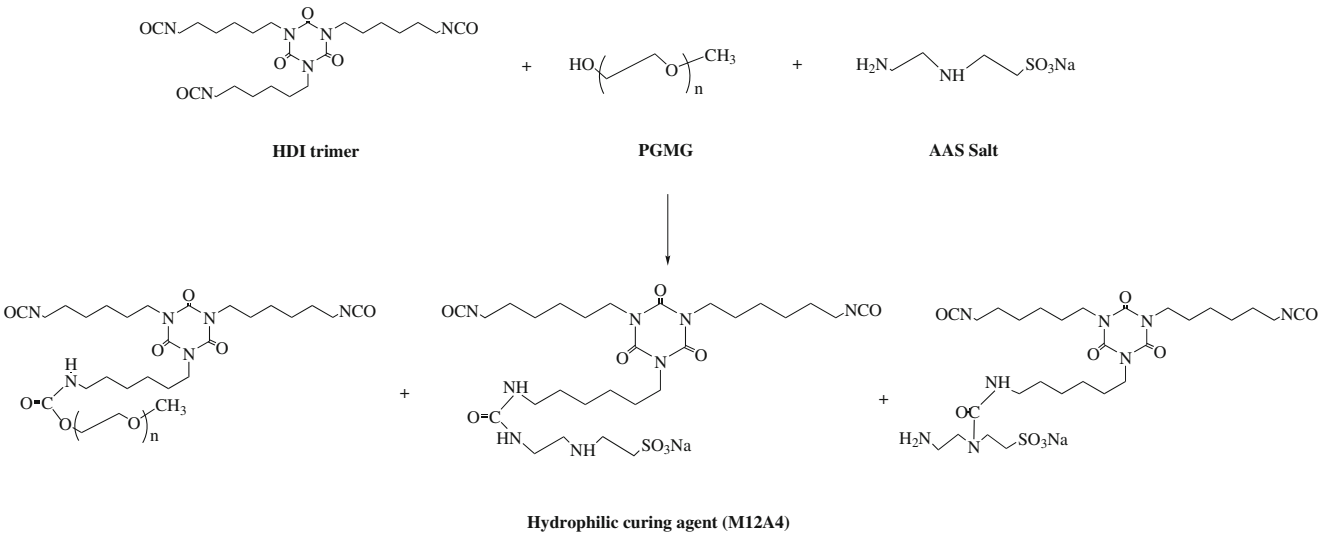

Scheme 1 Synthesis of hydrophilic curing agent

Where, V_1 represents the wasting volume of the standard solution of hydrochloric acid of vacuum testing in mL; V_2 represents the wasting volume of the standard solution of hydrochloric acid of hydrophilic curing agent in mL; c represents the actual concentration of the standard solution of hydrochloric acid in mol/L (this experiment used 1.0004 mol/L standard solution of hydrochloric acid); m represents the weight of hydrophilic curing agent in g; 0.00420 means equal to a 1.00 mL standard solution of hydrochloric acid concentration of which is $c_{(HCl)}$ = 1.000 mol/L.

The particle size and zeta potential of NOPUDs were determined at 25 °C with Nanosizer (Malvern zeta sizer Nano ZS90, Malvern Instruments Ltd., Malvern, England).

The 1.0 g hydrophilic curing agent was dispersed in 20 mL deionized water at 300 rpm mechanical stirring. The complex dispersal time was recorded (when no flocculent appeared). The pot life of the hydrophilic curing agent was recorded −NCO value for 1 day, 2 days, 1 week, 2 weeks, 1 month, 2 months, 3 months, 4 months, and 5 months.

Two-component waterborne polyurethane coatings and films

The films were cut to 25 × 25 × 2 mm quartz plates and then placed into a vacuum drying oven at 80 °C for 12 h. The Nicolet 8700 Fourier transformed infrared spectroscopy (FTIR, Thermo Nicolet Corporation, Waltham, USA) was used to test the films of the quartz plates.

The mechanical properties of films were tested using an electronic and mechanical testing machine (AGS-J electronic and mechanical testing machine, Japan Shimadzu Ltd. Co., Osaka, Japan).

The glass transition temperatures of films were tested through differential scanning calorimeter (Switzerland Mettler Toledo DSC 1 differential scanning calorimeter, Mettler-Toledo International Inc., Zurich, Switzerland). The measurements were tested at liquid nitrogen condition from − 100 to 150 °C at the warming speed 10 °C/min. The samples were dried at 80 °C for 24 h.

The thermal degeneration of films and char yield of coatings was tested through thermogravimetric analysis (Switzerland Mettler TGA/DSC differential thermal scanners, Mettler-Toledo International Inc., Zurich, Switzerland). The measurements were tested at nitrogen condition from 30 to 500 °C at a warming speed 10 °C/min. The samples were dried at 80 °C for 24 h.

The gaseous product from thermal degeneration of film was tested through thermogravimetric infrared analysis (Mettler Toledo TGA/DSC1-Ncolet 6700 FTIR, Mettler-Toledo International Inc., Zurich, Switzerland). The measurements were tested at nitrogen condition from 30 to 500 °C at a warming speed 10 °C/min. The samples were dried at 80 °C for 24 h.

The limiting oxygen index (LOI) of films was determined using the digital display oxygen index apparatus LFY-606B (Shandong textile science and technology, Jinan, China) via standard test ASTM D2863-77. The films were cut to 150 × 50 mm splines (each sample had five strips).

UL-94 of films was conducted by a CZF-II horizontal and vertical burning tester (Jiang Ning Analysis Instrument Co.). The specimens used were 150 × 50 × 2 mm according to the UL-94 tests (ASTM D3801-1996 standard).

Results and discussion

The novel hydrophilic curing agent and flame-retardant two-component waterborne polyurethanes were successfully synthesized.

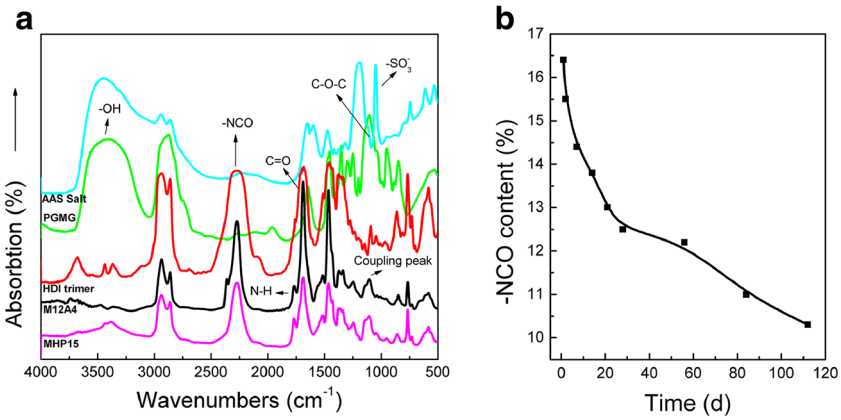

Fig. 1 FTIR (a) and pot life (b) of hydrophilic curing agent (M12A4)

Hydrophilic curing agent

In FTIR spectrum of HDI trimer and hydrophilic curing agents, the stretching vibration absorption of C=O are all at 1682 cm^{-1} (Fig. 1a). The absorption of −NCO of the HDI trimer and M12A4 at 2273 cm^{-1}, the stretching vibration absorption of N-H at 3343 cm^{-1}, and the absorption of −OH at 3400 cm^{-1} were weakened due to a reaction from PGMG or AAS salt. The in-plane bending absorption of N-H at 1551 cm^{-1} meant that −OH and −NCO successfully reacted. Besides, the overlapping peak of C-O-C at 1106 cm^{-1} was enhanced through adding PGMG because of producing more NH-C(O)-O-C. The symmetry and dissymmetry stretching vibration absorption of $-SO_3^-$ at 1090 and 1044 cm^{-1} coincided with the stretching vibration coupling peak of C-N and C-O at 1174 cm^{-1} and symmetry stretching vibration peak of N-CO-O and C-O-C at 1069 cm^{-1}, which showed a single peak [11, 12].

Frequently, denser particle concentration caused stronger interaction and larger viscosity in the emulsion [13, 14]. From Table 1, the viscosity and grain size of M12A4 were 80 mPa s and 210.8 nm, respectively; however, the viscosity and grain size of MHP15 were 90.7 mPa s and 132.7 nm [10]. One possible reason was that the intermolecular force between PGMG and AAS salt was stronger than that of HDI trimer, which increased viscosity. Another potential reason was linear structure of hydrophilic curing agent, which caused to increase molecular weight and entanglement through PGMG and AAS salt [15, 16]. Therefore, more PGMG and AAS salt led to smaller micelle to produce stronger intermolecular forces and higher viscosity. The zeta potential was − 30 mV which indicated M12A4 had satisfactory electrostatic stabilization [17]. Meanwhile, the −NCO content was 16.4%, which was larger than the threshold of 10.0% required to signify invalid agent. Hence, M12A4 had good emulsion stability pot life (Fig. 1b). During the first week, −NCO obviously decreased because of the remaining air in the storage bottle, which distinctly weakened the −NCO content. The water present in the air could react with the pure HDI trimer to damage the protection effect induced through the modified HDI trimer. After another week, the original decreasing trend slowly changed due to the modified HDI trimer being able to protect the inertial HDI trimer from the water present in air. The data revealed that the 4th month was the pot life of M12A4.

Emulsion properties of flame-retardant two-component waterborne polyurethane coatings

According to FTIR spectrum (Fig. 2), the stretching vibration absorption of C=O at 1685 cm^{-1} was according to carbamate. The absorption of P-C at 1461 cm^{-1}, absorption of P=O at 1259 cm^{-1}, vibration absorption of C-O of P-O-C at 1107 cm^{-1}, vibration absorption of P-O of P-O-C at 938 cm^{-1}, weak vibration absorption of P-C at 834 cm^{-1}, which were according to OP550 unit in main chain. The coupling peak of $-SO_3^-$, N-CO-O and C-O-C showed a single peak because of symmetry and dissymmetry stretching vibration absorption of $-SO_3^-$, stretching vibration coupling peak of C-N and C-O, and symmetry stretching vibration peak of N-CO-O and C-O-C.

Table 1 Grain size, zeta potential, viscosity, and mechanical properties of MWPU and MAWPU

Samples	Average grain size (nm)	Zeta potential (mV)	Viscosity (mPa·s)	Tensile Strength (MPa)	Fracture Elongation (%)
MWPU-1	195.0	− 32.2	20.1	11.3	335.8
MWPU-2	210.2	− 31.7	17.2	12.8	305.6
MAWPU-1	186.0	− 33.5	19.2	17.3	380.3
MAWPU-2	203.8	− 31.9	17.9	18.4	317.5

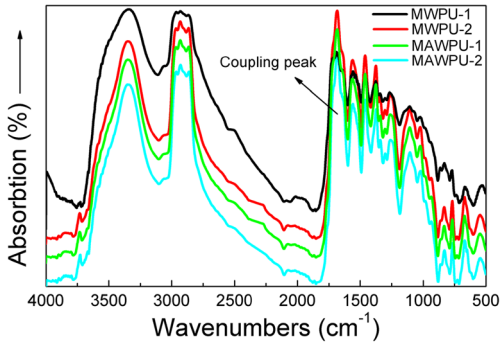

Fig. 2 FTIR of flame-retardant two-component waterborne polyurethanes

Then, the emulsion properties were analyzed here. Waterborne polyurethane latexes could exist stably because of the mutual repulsion caused through the micelle adsorbing electric double layer. Larger grain size, slower electrophoretic velocity, and a less positive ion absorbed micelle surface created a shorter zeta potential and weaker stability in the emulsion [18]. From Table 1, the average grain size and zeta potential of MAWPU was slightly less than that of MWPU at the same stoichiometric ratio of −NCO to −OH, which meant that MAWPU had better stability. One reason was that the molecule volume of $-SO_3^-$ was less than that of the ether bond. MAWPU had smaller volume because M12A4 with $-SO_3^-$ endowed MAWPU emulsion slightly better emulsion properties. The larger the absolute value of zeta potential signified better mechanical and chemical stability in the same condition [19, 20]. The two emulsions were both static stability emulsions because their zeta potentials were both less than − 30 mV. Emulsion viscosity was influenced through particle morphology and size. Hence, the viscosity of MAWPU was slightly larger than that of MWPU.

Mechanical testing

As can be seen in Table 1, the tensile strength of MAWPU was about 1.5 times than that of MWPU and the fracture elongation of MAWPU was over 12 even 44% larger than that of MWPU at the same stoichiometric ratio of −NCO to −OH. The reason was that $-SO_3^-$ and $-CH_2CH_2SO_3$ existed in the MAWPU macromolecule chain, which increased the relative molecular mass of the hard segment unit of polyurethane. Hence, the tensile strength of MAWPU was obviously larger than MWPU. The larger the numbers of small steric hindrance groups, the better the tensile strength [21, 22]. Consequently, M12A4 could more easily promote strong acing force than MHP15 among hard segments that was beneficial for forming lamella or microcrystalline structure.

Thermal behavior

Differential scanning calorimeter

The hydrophilic curing agent and two-component waterborne polyurethane both had two glass transition temperatures (T_g): the T_g of the hard segment (T_{gh}) and the T_g of the soft segment (T_{gs}), which meant that polyurethane excited obvious microphase separation [23]. Generally, the difference value (ΔT_g) between T_{gs} and T_{gh} could be utilized to characterize microphase separation in polyurethane. The soft segment showed kinetic characteristic of pure soft segment, which weakened the influence of the urethane hard segment created through hydroxide group and isocyanato [23]. Consequently, the T_{gs} of polyurethanes closed to the T_{gs} of the curing agent. From Fig. 3a and Table 2, the microphase separation of MAWPU was less than for MWPU, which meant that the compatibility between the soft and hard segments of MAWPU was better than MWPU. Therefore, the M12A4 had played a definite part in accelerating the compatibility between soft and hard segments.

Thermogravimetric analysis

The thermal degradation of MWPU-1 was performed according to a previous paper [10], and the thermal degradation of MWPU-2 was similar to that of MWPU-1. In this paper, the

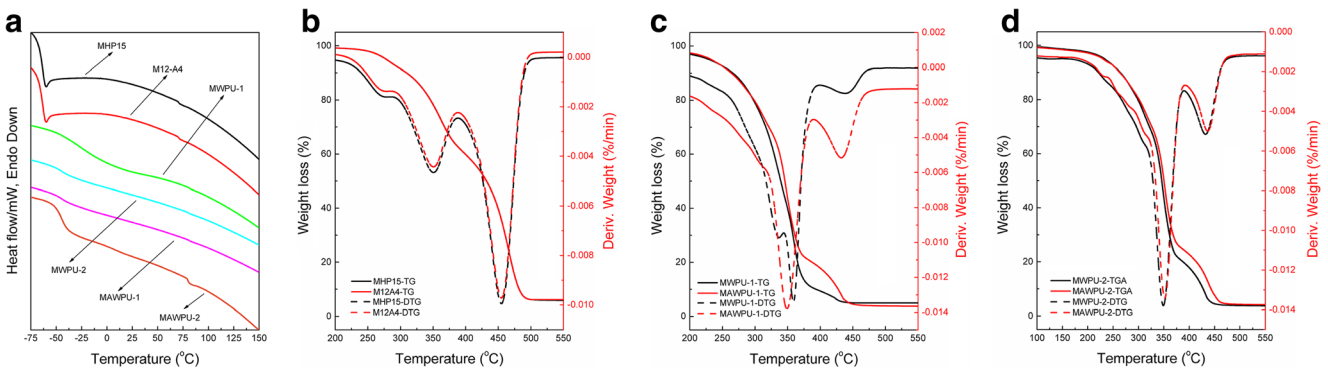

Fig. 3 DSC and TGA of hydrophilic curing agent, MWPU and MAWPU. **a** DSC. **b** TGA and DTG of hydrophilic curing agent. **c** TGA and DTG of MWPU-1 and MAWPU-1. **d** TGA and DTG of MWPU-2 and MAWPU-2

Table 2 The glass transition temperature (T_g), maximum degradation speed (V_{max}), and temperature (T_{max}) of coatings

Sample	T_{gs}	T_{gh}	$\triangle T_g$	1st stage		2nd stage		3rd stage		4th stage	
				T_{max} (°C)	V_{max} (%/°C)	T_{max} (°C)	V_{max} (%/°C)	T_{max} (°C)	V_{max} (%/°C)	T_{max} (°C)	V_{max} (%/°C)
MHP15	− 65.7	72.4	138.1	263	4.2635	321	0.0020	418	0.0063	–	–
M12A4	− 65.8	71.8	137.6	263	4.2623	329	0.0019	419	0.0062	–	–
MWPU-1	− 42.0	81.0	123.0	305	0.0101	357	0.0065	440	0.0015	–	–
MWPU-2	− 45.1	80.8	125.9	228	0.0023	350	0.0138	431	0.0052	–	–
MAWPU-1	− 42.6	80.2	122.8	233	0.0014	305	0.0039	350	0.0126	431	0.0038
MAWPU-2	− 44.2	79.9	124.7	230	0.0019	309	0.0039	351	0.0123	440	0.0040

MAWPU and the difference between MWPU and MAWPU were analyzed in detail. From Fig. 3c to 3d, the thermal degradation of MAWPU was divided into four stages. The first stage occurred between 180 to 245 °C, and the maximum degradation temperature (T_{max}) of this stage was about 230 °C. The second thermal degradation started at 245 °C, where there was thermal degradation of the sulfonate group and organic phosphate. The third stage occurred the degradation of hard segment from 324 °C [23, 24]. Finally, the last stage started from 391 to 480 °C. From Table 2, comparing with MWPU, the maximum degradation speed of the hard and soft segment (V_{max}) in MAWPU was almost lower with higher stoichiometric ratio of −NCO to −OH, which meant that M12A4 could restrain the degradation speed. Meanwhile, M12A4 could increase T_{max} of each thermal degradation stage because the sulfonate group was decomposed to produce SO_2. The synergistic effect between the SO_2 and phosphate groups produced at the second stage could accelerate the production of carbon layers and prohibit the growth of energy [21, 25]. Additionally, the thermal degradation of MWPU and MAWPU coatings was unchanged at 500 °C, which meant that MWPU and MAWPU decomposed completely. Therefore, 500 °C was considered the complete degradation temperature.

Thermal degradation mechanisms

Gaseous decomposition

According to the 3D-TGA-FTIR image presented in Fig. 4a, infrared absorption spectrums of released gas were obtained at different decomposed (Fig. 4b). The sample also had four gas emission stages, which was consistent with TGA. The first was at 180 °C, which had a small amount of gases. The absorption of methyl or methylene groups from 2979 to 2885 cm^{-1}, the absorption of carboxylate at 1659 cm^{-1}, derived from decomposition of neutralization chain. Therefore, the M12A4 could delay the gas evolution during decomposition (Fig. 4c). The second release of gases occurred between 245 and 324 °C. The third stage included large amounts of gases between 324 and 391 °C, and the fourth also released large amounts of gases after 391 °C. In further exploration, an analysis was conducted to determine the molecular structure of the released gases.

Thermal degradation mechanism

The thermal degradation mechanism of MWPU and MAWPU is summarized according to TGA-FTIR. Firstly, neutralization

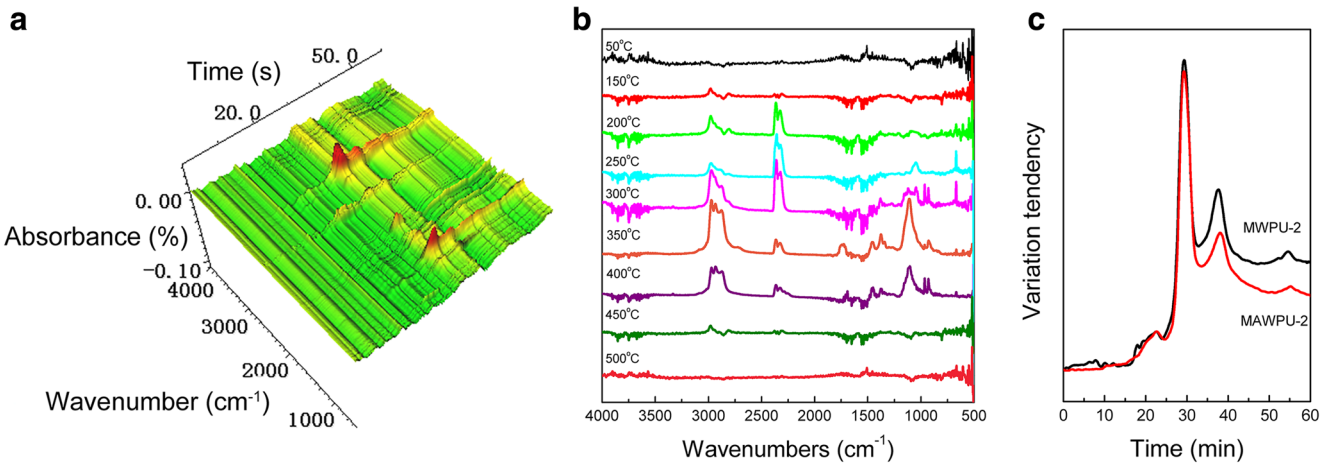

Fig. 4 TGA-FTIR three-dimensional spectrum, FTIR of released gas decomposed, and variation of gas evolution. **a** Three-dimensional spectrum. **b** FTIR. **c** Variation of gas evolution

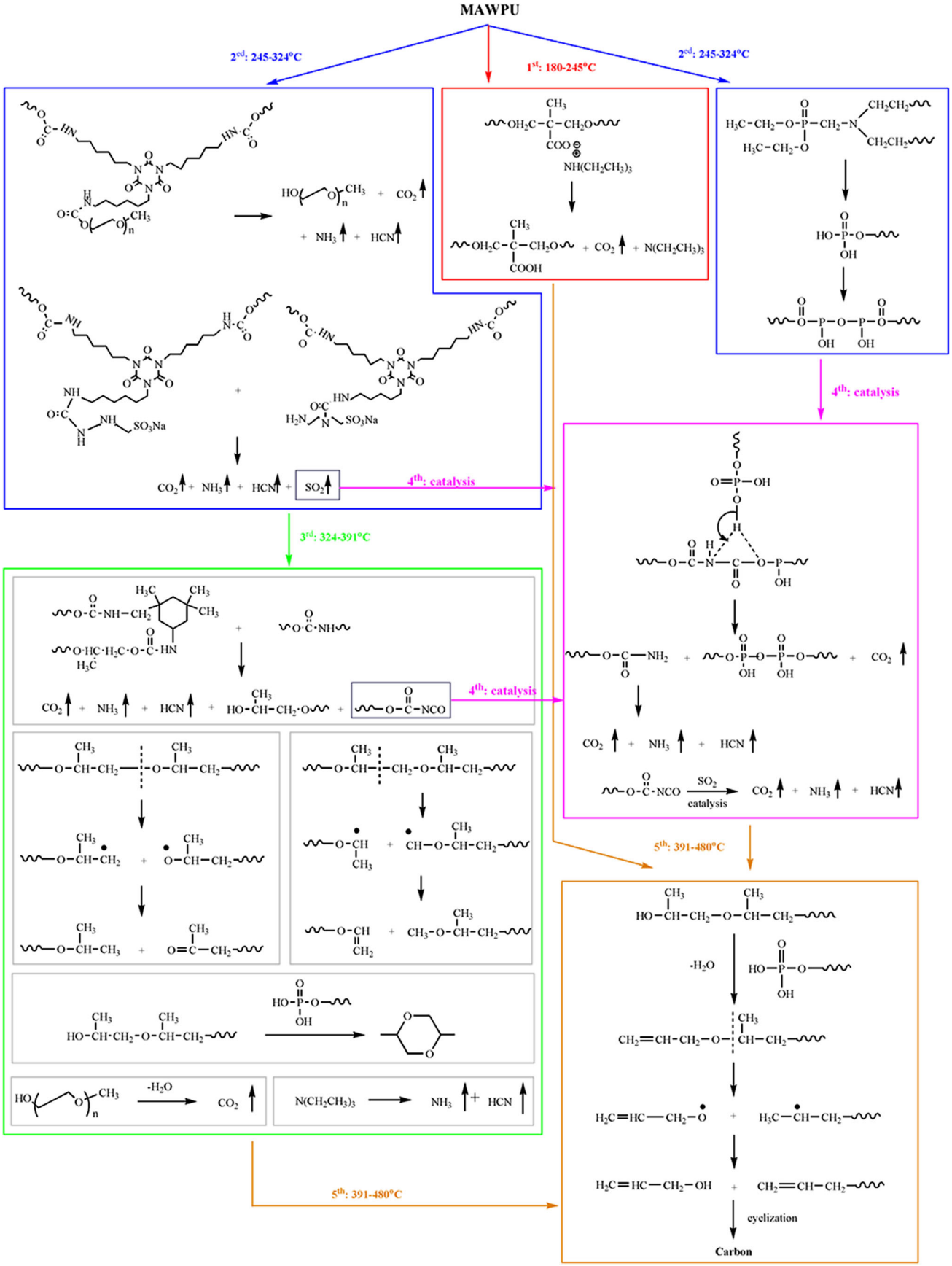

Scheme 2 The thermal degradation mechanism mode of MAWPU coatings

Table 3 LOI value, carbon yield, and UL-94 testing results

Sample	LOI value (%)	Carbon yield (%)	UL-94 (level)
MWPU-1	28.6	4.79	V-0
MWPU-2	28.0	3.85	V-1
MAWPU-1	28.7	3.88	V-1
MAWPU-2	29.4	4.28	V-0

chain was depredated to produce CO_2 between 180 and 245 °C. Secondly, sulfonate group and organic phosphate of MWPU and MAWPU were degraded between 245 and 324 °C to produce SO_2 and phosphate groups (phosphoric acid and polyphosphoric acid). Thirdly, the thermal degradation of the hard segment of MWPU and MAWPU occurred between 324 and 391 °C. SO_2 and phosphate groups promoted the degradation of the third stage to produce polyether main chains and volatilize nonflammable gases such as CO_2, HCN, and NH_3. Finally, the soft segment was decomposed between 391 and 480 °C. Soft segment was decomposed to create a small molecule ether, ketone, aldehyde, and carbon through phosphate groups (phosphoric acid and polyphosphoric acid). Meanwhile, residual hard segment was further decomposed to NH_3 [26, 27]. The specific thermal decomposition mechanism mode was organized in Scheme 2.

Flame retardancy

The LOI value, carbon residue yield, and UL-94 testing results of MWPU and MAWPU are listed in Table 3. The LOI value was the most important index for measuring the material flame retardancy. It is generally thought that materials with a LOI value of less than 22% are highly inflammable; LOI values of between 22 and 27% are combustible materials, LOI of greater than 27% are nonflammable materials, and LOI values of greater than 32% are non-combustible materials [28]. As seen in Table 3, the LOI values of MAWPU were over 28.7% and larger than that of MWPU. The reason was the promotion of SO_2. Meanwhile, carbon yield became larger with more sulfonate group. The nonflammable carbon layers covered the surface of polymer to barrier oxygen outside, and then interrupted combustion chain reaction to delay combustion speed of the whole materials [29]. The UL-94 testing results showed that MAWPU was improved through sulfonate group to reach V-0 level, while MWPU was declined to V-I level via adding more MHP15. This indicated that MAWPU belonged to nonflammable materials and had better flame retardancy. The decomposed production of sulfonate group could create a certain cladding on the surface of two-component waterborne polyurethanes (Fig. 3). The cladding layer controlled the energetic growth which declined the energy density and prevented surface heat transmission from combustible gas in the matrix during burning [30]. Sulfonate group accelerated the condensed-phase flame retardancy in two-component waterborne polyurethane to improve flame retardancy.

Conclusions

The paper successfully synthesized a novel hydrophilic curing agent, which could improve tensile strength, compatibility, and flame retardancy of flame-retardant two-component waterborne polyurethanes. Meanwhile, MWPU and MAWPU showed nice emulsion stability. Meanwhile, the maximum degradation speed of MAWPU was lower than in MWPU due to catalysis of SO_2 which also increase maximum degradation temperature. The sulfonate group could effectively inhibit decomposition and effectively created condensed-phase flame retardancy with OP550 during burning.

Acknowledgements Supported through the National Key Research and Development Program of China (2016YFC0204400).

Conflict of Interest The authors declare that they have no conflict of interest.

References

1. Akbarian M, Olya ME, Ataeefard M, Mahdavian M (2012) The influence of nanosilver on thermal and antibacterial properties of a 2K waterborne polyurethane coating. Progress in Organic Coatings 75(4):344–348. https://doi.org/10.1016/j.porgcoat.2012.07.017
2. Ge Z, Luo Y (2013) Synthesis and characterization of siloxane-modified two-component waterborne polyurethane. Progress in Organic Coatings 76(11):1522–1526. https://doi.org/10.1016/j.porgcoat.2013.06.007
3. Wu G, Li J, Chai C, Ge Z, Lin J, Luo Y (2015) Synthesis and characterization of novel post-chain extension flame retardant waterborne polyurethane. RSC Adv 5(118):97710–97719. https://doi.org/10.1039/c5ra12975c
4. Alcón MJ, Ribera G, Galià M, Cádiz V (2005) Advanced flame-retardant epoxy resins from phosphorus-containing diol. J Polym Sci A Polym Chem 43(16):3510–3515. https://doi.org/10.1002/pola.20856
5. Geurink PJA, Scherer T, Buter R, Steenbergen A, Henderiks H (2006) A complete new design for waterborne 2-pack PUR coatings with robust application properties. Prog Org Coat 55(2):119–127. https://doi.org/10.1016/j.porgcoat.2005.08.014
6. Jacobs Patricia B. PTA (1992) Water dispersible polyisocyanates. CA2088311A1
7. Karl H (1994) Water-emulsifiable polyisocyanates. CA2158621A1,
8. Luo Y, Yin X, Chai C, Ge Z (2017) A kind of mixed hydrophilic polyisocyanate curing agent and its preparation method
9. Yin X, Luo Y, Zhang J (2017) Synthesis and characterization of halogen-free flame retardant two-component waterborne polyurethane by different modification. Ind Eng Chem Res 56(7):1791–1802. https://doi.org/10.1021/acs.iecr.6b04452

10. Birowosuto MD, Takiguchi M, Olivier A, Tobing LY, Kuramochi E, Yokoo A, Hong W, Notomi M (2017) Temperature-dependent spontaneous emission of PbS quantum dots inside photonic nanostructures at telecommunication wavelength. Opt Commun 383: 555–560. https://doi.org/10.1016/j.optcom.2016.09.059
11. Wu Guomin KZ, Caifeng C, Jian C, Shuping H, Jianchun J (2013) Crosslinking reaction and properties of two-component waterborne polyurethane from terpene-maleic ester type epoxy resin. J Appl Polym Sci 128:132–138. https://doi.org/10.1002/app.38130
12. Chagnon L, Arnold G, Giljean S, Brogly M (2013) Elastic recovery and creep properties of waterborne two-component polyurethanes investigated by micro-indentation. Prog Org Coat 76(10):1337–1345. https://doi.org/10.1016/j.porgcoat.2013.04.003
13. Lee H, Wu S, Jeng R (2006) Effects of sulfonated polyol on the properties of the resultant aqueous polyurethane dispersions. Colloids Surf A Physicochem Eng Asp 276(1–3):176–185. https://doi.org/10.1016/j.colsurfa.2005.10.034
14. Tawa T, Ito S (2004) Preparation and reactions of hydrophilic isocyanate micelles dispersed in water. Colloid Polym Sci 283(7):731–737. https://doi.org/10.1007/s00396-004-1213-1
15. Orgilés-Calpena E, Arán-Aís F, Torró-Palau AM, Orgilés-Barceló C, Martín-Martínez JM (2009) Addition of different amounts of a urethane-based thickener to waterborne polyurethane adhesive. Int J Adhes Adhes 29(3):309–318. https://doi.org/10.1016/j.ijadhadh.2008.06.004
16. Cakic SM, Stamenkovic JV, Djordjevic DM, Ristic IS (2009) Synthesis and degradation profile of cast films of PPG-DMPA-IPDI aqueous polyurethane dispersions based on selective catalysts. Polym Degrad Stab 94(11):2015–2022. https://doi.org/10.1016/j.polymdegradstab.2009.07.015
17. Pérez-Limiñana MA, Arán-Aís F, Torró-Palau AM, César Orgilés-Barceló A, Miguel Martín-Martínez J (2005) Characterization of waterborne polyurethane adhesives containing different amounts of ionic groups. Int J Adhes Adhes 25(6):507–517. https://doi.org/10.1016/j.ijadhadh.2005.02.002
18. Redfern JP (1999) Property evaluation of FR polymeric materials using a range of instrumental techniques. Polym Degrad Stab 64: 561–572
19. Myers D (1999) Surfaces, interfaces, and colloids. Principles and Applications (2nd ed). John Wiley & Sons, Inc.
20. Shaw D (1992) Introduction to colloid and surface chemistry (4th ed). Elsevier Ltd
21. Hwang S-s, Hsu PP (2013) Effects of silica particle size on the structure and properties of polypropylene/silica composites foams. J Ind Eng Chem 19(4):1377–1383. https://doi.org/10.1016/j.jiec.2012.12.043
22. Jiang L, Spearing SM, Monclus MA, Jennett NM (2011) Formation and mechanical characterisation of SU8 composite films reinforced with horizontally aligned and high volume fraction CNTs. Compos Sci Technol 71(10):1301–1308. https://doi.org/10.1016/j.compscitech.2011.04.017
23. Cho BS, Kim JS, Lee JM, Kweon JO, Noh ST (2014) Synthesis and characterization of poly(ferrocenyl glycidyl ether)-1,2-butylene oxide copolymers. Macromol Res 22(8):826–831. https://doi.org/10.1007/s13233-014-2115-9
24. Lee HS, Hsu SL (1989) An analysis of phase separation kinetics of model polyurethanes. Macromolecules 22(3):1100–1105
25. Tjong SC (2006) Structural and mechanical properties of polymer nanocomposites. Mat Sci Engi: R: Rep 53(3–4):73–197. https://doi.org/10.1016/j.mser.2006.06.001
26. Youssef B, Lecamp L, Khatib WE, Bunel C, Mortaigne B (2003) New phosphonated methacrylates: synthesis, photocuring and study of their thermal and flame-retardant properties. Macromol Chem Phys 204(15):1842–1850. https://doi.org/10.1002/macp.200300025
27. van der Schuur M, Noordover B, Gaymans RJ (2006) Polyurethane elastomers with amide chain extenders of uniform length. Polymer 47(4):1091–1100. https://doi.org/10.1016/j.polymer.2005.11.074
28. Du L, Qu B, Xu Z (2006) Flammability characteristics and synergistic effect of hydrotalcite with microencapsulated red phosphorus in halogen-free flame retardant EVA composite. Polym Degrad Stab 91(5):995–1001. https://doi.org/10.1016/j.polymdegradstab.2005.08.004
29. Gallagher S (2003) Synthesis and characterization of phosphonate-containing polysiloxanes. J Polym Sci: Part A: Polym Chem 41:48–59
30. Cho J, Joshi MS, Sun CT (2006) Effect of inclusion size on mechanical properties of polymeric composites with micro and nano particles. Compos Sci Technol 66(13):1941–1952. https://doi.org/10.1016/j.compscitech.2005.12.028